

# Design and operation of a spark chamber for vacuum ultraviolet light production

Silas Bosco<sup>1</sup>, Jonas Bürgi<sup>1</sup> , Livio Calivers<sup>1</sup> , Richard Diurba<sup>1</sup> , Johannes Furrer<sup>1</sup> , Jan Kunzmann<sup>1</sup> , Saba Parsa<sup>1</sup> , Sascha Rivera<sup>1</sup>, Nicolas Sallin<sup>1</sup> , Camilla Tognina<sup>1</sup>, Serhan Tufanli<sup>1\*</sup>, Michele Weber<sup>1</sup> , Dominik Wermelinger<sup>1</sup> 

<sup>1</sup> Laboratory for High Energy Physics, Albert Einstein Center for Fundamental Physics, Universität Bern, 3012 Bern, Switzerland

\* Correspondence: serhan.tufanli@unibe.ch

## Abstract

Noble liquids, notably argon and xenon, are utilised as both detector media and as the detector target for dark matter and neutrino physics experiments. When the noble liquid is excited by particles, it scintillates vacuum ultraviolet light, which sensors then detect. A major focus of the detector development community is on producing precision light sensors for noble liquid detectors. We introduce a flash lamp to test light sensors with light at wavelengths observed at noble liquid detectors. This paper discusses the design and presents results from a spark chamber prototype operated at room temperature.

**Keywords:** noble liquid scintillation light, detector development

## 1. Introduction

Argon and xenon-based detector technologies are utilised by many neutrino and dark matter experiments [1–6]. The excitation of the detector medium by particles generates prompt scintillation light via argon-excimer de-excitation, yielding photons in the vacuum ultraviolet (VUV). For argon, this light has a peak wavelength at 128 nm [7]. Experiments surround the detector material with light sensors to maximise signal detection. The light detection signals from the sensors are then used to identify and characterise particles in the medium.

Direct tests in noble liquids reproduce the desired spectrum but are time- and infrastructure-intensive as they require cryogenic systems. Test setups for light sensors rely on light-emitting diodes (LEDs), whose spectra do not extend into the VUV. Improvements have been made to provide VUV light without significant infrastructure at relevant wavelengths with deuterium lamps, such as Nikhef's VULCAN system [8]. However, these commercial lamps produce spark emission and quasi-constant light, which is not ideal for signal-shaping or single-photoelectron performance studies. These limitations highlight the need for a room-temperature device that promptly produces VUV photons with high spectral purity. An example of such an argon lamp is presented in Reference [9].

We have designed an argon flash lamp, a compact apparatus that exploits electrical discharges in argon gas to generate VUV light through the same excimer processes occurring in the liquid phase. The lamp is intended to be portable and flexible to changes in electrode distance and gas pressure, while enabling precise, repeatable characterisations of photosensors for noble element detectors. The testing setup proposed here also produces light pulses on the  $\mu\text{s}$ -timescale to allow the data acquisition system to synchronise timing

Received:  
Revised:  
Accepted:  
Published:

**Copyright:** © 2026 by the authors.  
Submitted to *Instruments* for possible open access publication under the terms and conditions of the [Creative Commons Attribution \(CC BY\)](https://creativecommons.org/licenses/by/4.0/) license.

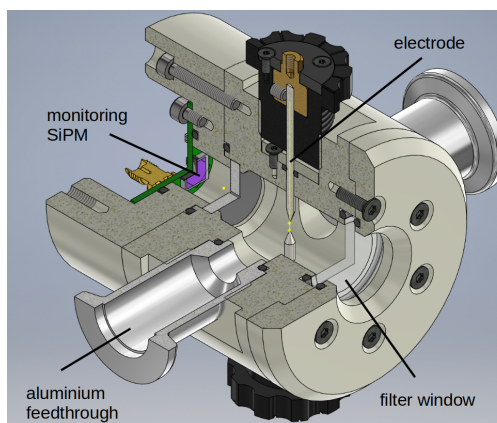


**Figure 1.** Diagram of the flash lamp chamber with an interior view of the electrodes and filter.

between the lamp and light sensors. This paper describes the design and operation of the flash lamp.

## 2. Design of the Argon Flash Lamp

The sparking chamber is the core of the argon flash lamp. The chamber is a cylindrical vessel 65 mm in diameter and 73 mm tall, machined from poly-ether-ether-ketone (PEEK). This high-performance thermoplastic offers exceptional electrical insulation, chemical inertness, and mechanical strength. Its low outgassing rate and dimensional stability across a broad temperature range make PEEK especially well-suited for vacuum and high-voltage environments, permitting precise electrode alignment and reliable operation through repeated discharge cycles.

A diagram of the chamber is shown in Figure 1, with Figure 2 showing diagrams from the side and front views of the chamber. Two aluminium feedthroughs are integrated into the sidewall. High-purity argon travels through these aluminium feedthroughs. VUV light flashes are produced between a pair of opposing electrodes positioned at the top and bottom of the chamber and aligned along the central axis, as shown in Figure 2. The electrodes can be in contact, and the rotary mechanism allows for their distance to increase in 0.1 mm increments to a maximum separation of 10 mm. The internal parts of the rotary adjustment mechanism are fabricated from copper to ensure excellent conductivity. The assembly is sealed with O-rings to maintain vacuum integrity while providing smooth rotation and electrical isolation from the chamber body.

A monitoring SiPM connected to a printed circuit board (PCB) is installed on one side of the chamber. This SiPM is inside the chamber to monitor flash synchronisation and light production. On the opposite side of the chamber from the monitoring SiPM, a filtering window is covered with a P/N 25125FNB VUV-Optical Filter produced by eSource Optics [10]. The filter allows only light within the narrow range of  $125 \text{ nm} \pm 2.5 \text{ nm}$ , corresponding to the emission from argon excimer decays. The light travels through the filtering window to exit the chamber. Only  $10^{-3}$  to  $10^{-4}$  of light with wavelengths greater than 127.5 nm or less than 122.5 nm is transmitted through the filter, significantly reducing non-VUV light emitted from the chamber.

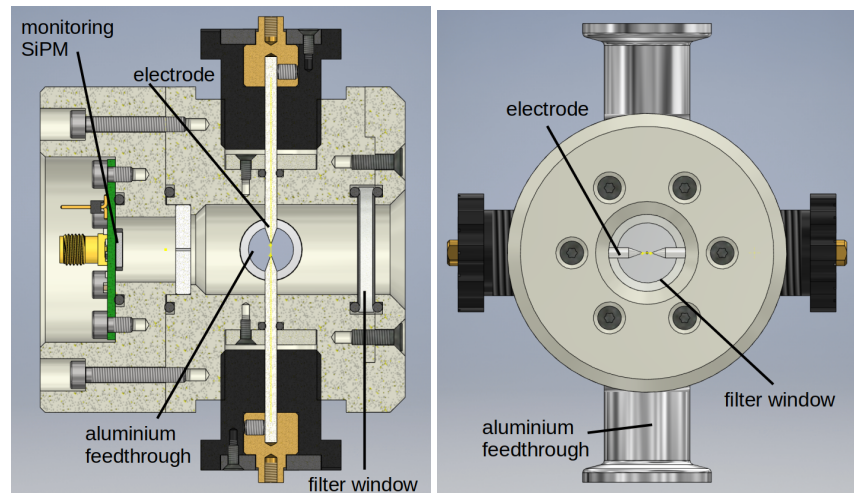


**Figure 2.** Diagram of the flash lamp chamber, looking at it from the side (left) and front (right) of the device.

The electrical circuit consists of two parts: a low-voltage regulator and a high-voltage discharge system, as shown in Figure 3. These two systems are connected via the Input/Output Proportional High Voltage Power Supply produced by Matsusada Precision [11], which provides the regulated high voltage needed for the discharge system.

The low-voltage regulator works as an adjustable linear voltage regulator. It produces a stable and controllable output voltage from a higher unregulated input supply of +20 V, unaffected by the unstable input voltage or the changing output load.

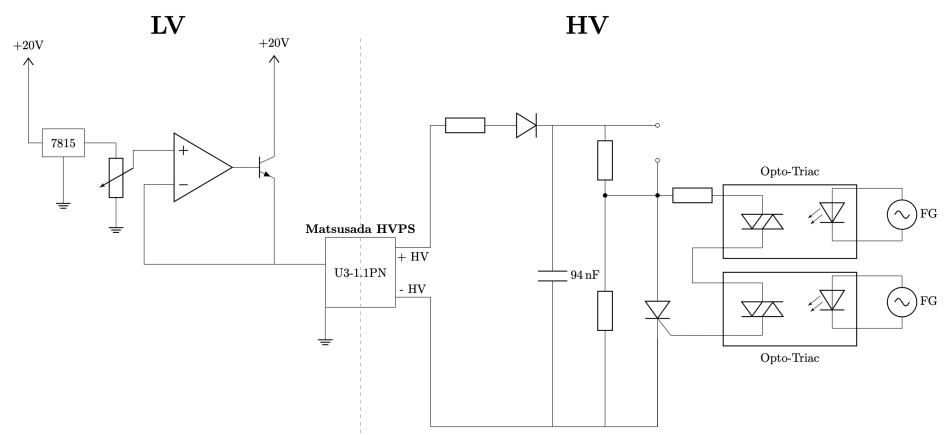


**Figure 3.** Diagram of the electrical circuit for the spark generation. The circuit consists of two parts: the first part is the low voltage (LV), and the second part is the high voltage (HV).

The high voltage discharge system is a capacitor-discharge circuit that delivers controlled sparks. The energy is stored in a bank of capacitors across the electrode gap, not shown in Figure 3. The two capacitors in the bank have a total capacitance of  $\approx 100 \mu\text{F}$ . The energy stored can be released in a microsecond-scale pulse over a gap that is adjustable to change the intensity of the spark. The voltage on the electrodes is set with a resistive voltage divider. A thyristor gate drives the lower-potential electrode momentarily to ground. An external function generator sets the gate width and the repetition rate.

### 3. Light Spectrum of the Flash Lamp

First, we validated the emission spectrum produced by the spark chamber. An Ocean Optics QEPro spectrometer (200 nm–1000 nm) recorded the light emission spectrum. For

this test, the optical filter window was replaced with an acrylic window to allow both VUV and non-VUV light to reach the spectrometer. The resulting intensity curve was normalised, and then an algorithm was applied for peak identification using the NIST Atomic Spectra Database [12]. The list is restricted to wavelengths between 200 nm and 1000 nm. We observed signals from the spectrometer associated with argon, hydrogen, nitrogen, and oxygen. Emissions from trace hydrocarbons, copper, aluminium, and iron originating from the chamber were considered negligible.

Each catalogue line was labelled with its element and ionisation stage (e.g., Ar I, O II) and the measured peaks were matched to the nearest reference line within a wavelength range of  $\pm 0.2$  nm. If multiple candidates were found inside this window, the match was considered ambiguous. The four defined categories are:

- Argon match: This peak corresponds to a wavelength peak of argon.
- Ambiguous with argon: There is an argon wavelength peak known within the tolerance of  $\pm 0.2$  nm at a wavelength shared with oxygen, nitrogen, and hydrogen.
- Ambiguous without argon: There are multiple candidates within the tolerance of  $\pm 0.2$  nm, and none of them is associated with argon.
- Non-argon match: This peak corresponds to another element.

Figure 4 shows the spectrum that was recorded over two seconds with a sparking frequency of 10 Hz, a spark gap of 1.8 mm, and a pressure of 4.5 mbar of argon. In total, for Figure 4, 19 wavelength peaks were detected, with 13 assigned uniquely to argon, two determined as ambiguous with argon, two peaks classified as unassigned without an overlapping argon emission peak, and the remaining two peaks assigned to other elements. The dominance of argon lines confirms that the present configuration successfully reproduces discharges that produce light at wavelengths associated with argon.

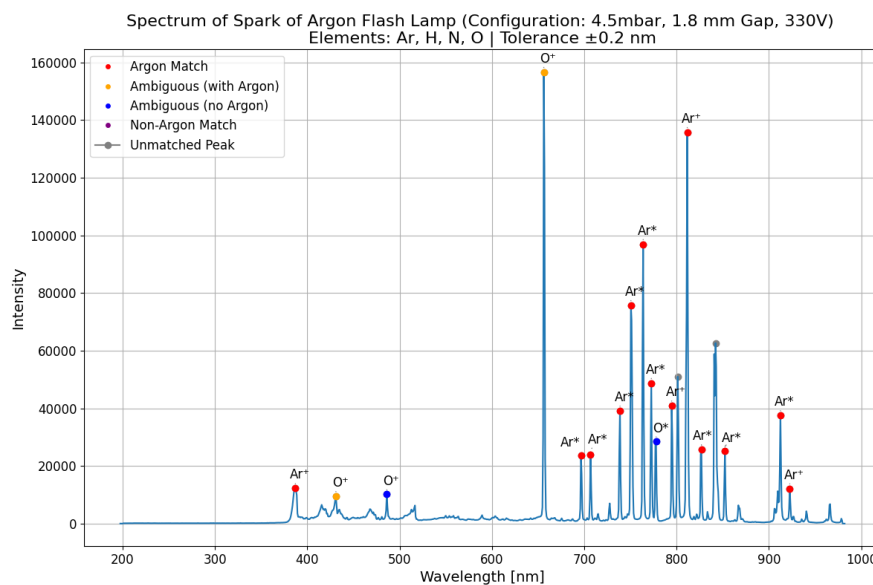


**Figure 4.** Spectrum of light collected over two seconds of pulsed sparking between two electrodes. The electrodes were at a distance of 1.8 mm at a frequency of 10 Hz, while the chamber had argon at a pressure of approximately 4.5 mbar. The identified elements of the peaks are labelled.

#### 4. Determination of VUV Emission

We performed a test to validate the device's applicability for testing SiPMs with VUV light. The spark was triggered across a distance of approximately 0.1 mm, and the filtering window was installed to only transmit light in the narrow range of  $125 \text{ nm} \pm 2.5 \text{ nm}$ . All

the other wavelengths are filtered by a factor of  $10^{-3}$ – $10^{-4}$  [10]. The filtering window was installed at the external side of the lamp, as shown in Figure 2.

Two test SiPMs were mounted on the external side, a few millimetres from the window on the outside of the chamber. Of the two SiPMs mounted, one is a Hamamatsu SiPM (S13360-6050CS) that is sensitive to 270 nm to 900 nm, and the other is a Hamamatsu VUV-sensitive SiPM (S13370) that is sensitive to light with wavelengths from 120 nm to 900 nm. Both the standard and VUV-sensitive SiPMs were connected to an oscilloscope for the analysis of their waveforms. The result of this measurement is shown in Figure 5. As can be seen, signals on both SiPMs were observed in time with the spark creation. The VUV-sensitive SiPM observed a higher voltage output, indicating that it detected a higher signal peak when compared to the non-VUV-sensitive SiPM. We note that there is a volume of air between the chamber and the SiPM. The VUV light interacting with air may lead to spectral contamination from UV and visible light.

To confirm the filtering of extraneous light, an additional test was made with an added layer of wavelength-shifting TPB placed in front of the SiPMs. The TPB layer is exposed to the transmitted light from the filter and shifts the light to wavelengths corresponding to visible light. The ratio of light detected by the VUV SiPM and the normal SiPM before and after adding a layer of TPB in front of the visible light SiPM further tests the production of VUV light. The ratio between the SiPM signals indicates that the non-VUV-sensitive SiPM detected more light when including the wavelength shifter, as seen in Figure 6. A final test, shown in Figure 7, was completed to cover the entire window outside of the chamber and confirm that signals observed by the SiPMs external to the flash lamp were due to the flash lamp and not due to noise.

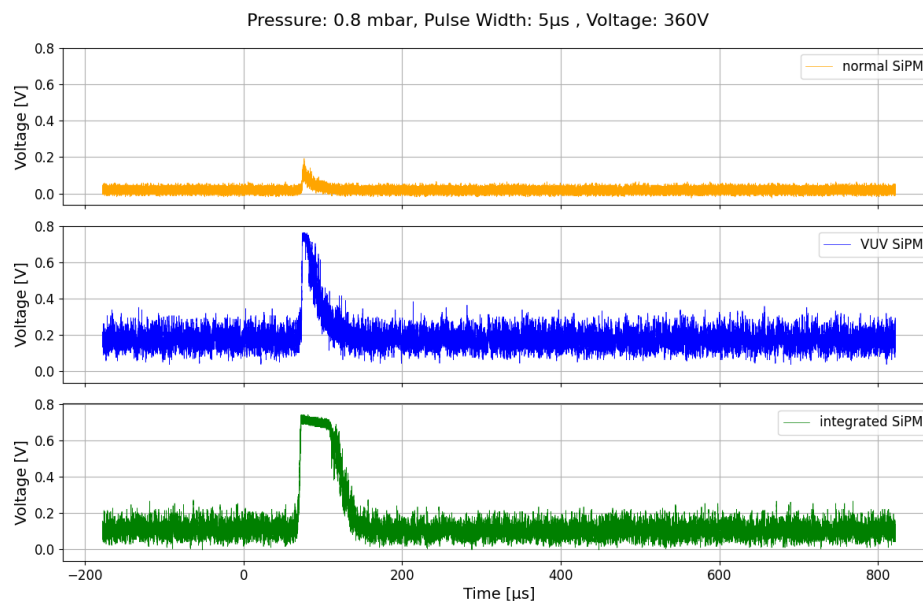


**Figure 5.** Measurements of light from the flash lamp without a filter in the filtering window for the normal and VUV-sensitive SiPMs. The SiPM optimised for visible light detected less light than the saturated VUV-sensitive SiPM.

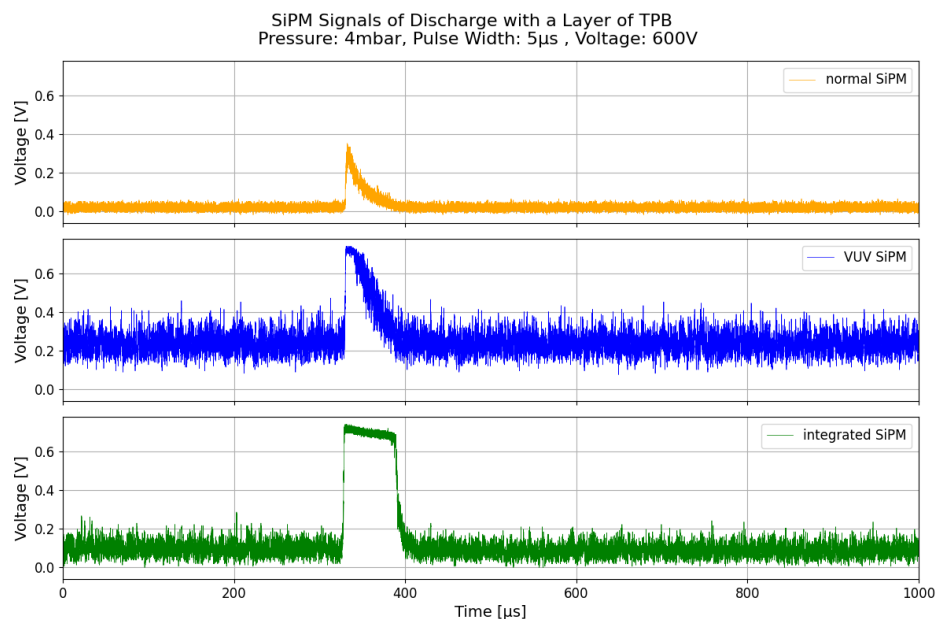


**Figure 6.** Measurements of light from the flash lamp. The filtering window was covered by a dichroic mirror with TPB to shift the produced light to the visible spectrum.

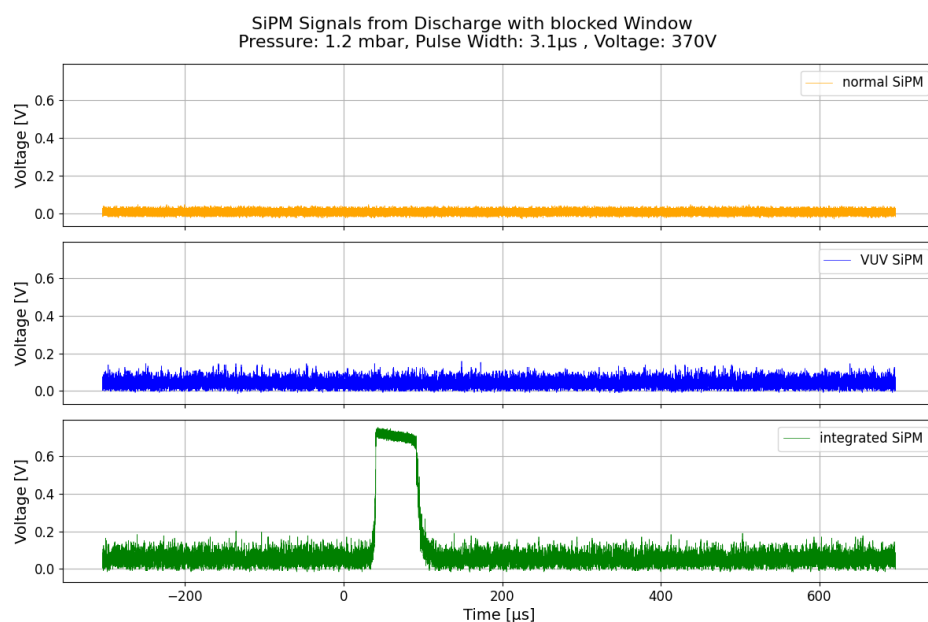


**Figure 7.** Measurements of light from the flash lamp. The filtering window was completely covered for this test, only allowing light to go to the monitoring SiPM.

## 5. Conclusion

We successfully built and tested a compact, flexible, and easy-to-operate VUV flash lamp. We demonstrated triggered discharges across an adjustable spark gap in argon gas. The measured emission spectrum shows good agreement with the known argon emission lines in the 200 nm–1000 nm range. Results indicate the production of VUV light by the spark chamber through cross-comparison measurements using a filtering window with a standard SiPM and a VUV-sensitive SiPM.

To reduce the probability of light sensor saturation, future studies will investigate reducing the intensity of light produced by exploring different electrode gaps. Additionally, further investigations are required to understand how the air gap between the SiPMs and

the chamber affects the spectrum of light reaching the sensors. Finally, the presented setup and measurements could be repeated with other noble elements, specifically xenon, to explore applications in other noble element-based particle physics experiments.

**Acknowledgments:** The research is funded by the Swiss National Science Foundation and by the Canton of Bern, Switzerland through grant 200020-204241. The study was supported by the Mechanic and Electronics Workshop at the Laboratory for High Energy Physics, Universität Bern, as well as the Albert Einstein Center for Fundamental Physics, Universität Bern.

**Conflicts of Interest:** The authors declare no conflicts of interest.

## References

1. Abi, B.; et al. Deep Underground Neutrino Experiment (DUNE), Far Detector Technical Design Report, Volume I Introduction to DUNE. *JINST* **2020**, *15*, T08008, [arXiv:physics.ins-det/2002.02967]. <https://doi.org/10.1088/1748-0221/15/08/T08008>.
2. Hewes, V.; et al. Deep Underground Neutrino Experiment (DUNE) Near Detector Conceptual Design Report. *Instruments* **2021**, *5*, 31, [arXiv:physics.ins-det/2103.13910]. <https://doi.org/10.3390/instruments5040031>.
3. Amaudruz, P.A.; et al. Design and Construction of the DEAP-3600 Dark Matter Detector. *Astropart. Phys.* **2019**, *108*, 1–23, [arXiv:astro-ph.IM/1712.01982]. <https://doi.org/10.1016/j.astropartphys.2018.09.006>.
4. Aalseth, C.E.; et al. DarkSide-20k: A 20 tonne two-phase LAr TPC for direct dark matter detection at LNGS. *Eur. Phys. J. Plus* **2018**, *133*, 131, [arXiv:physics.ins-det/1707.08145]. <https://doi.org/10.1140/epjp/i2018-11973-4>.
5. Aprile, E.; et al. The XENONnT dark matter experiment. *Eur. Phys. J. C* **2024**, *84*, 784, [arXiv:physics.ins-det/2402.10446]. <https://doi.org/10.1140/epjc/s10052-024-12982-5>.
6. Akerib, D.S.; et al. The LUX-ZEPLIN (LZ) Experiment. *Nucl. Instrum. Meth. A* **2020**, *953*, 163047, [arXiv:physics.ins-det/1910.09124]. <https://doi.org/10.1016/j.nima.2019.163047>.
7. Doke, T.; Hitachi, A.; Kikuchi, J.; Masuda, K.; Okada, H.; Shibamura, E. Absolute Scintillation Yields in Liquid Argon and Xenon for Various Particles. *Japanese Journal of Applied Physics* **2002**, *41*, 1538. <https://doi.org/10.1143/JJAP.41.1538>.
8. van Nuland-Troost, M.; Gupta, V.; Pollmann, T. VULCAN: Vacuum ultraviolet light characterisation at Nikhef. *Il Nuovo Cimento* **2024**, *47*, 378. <https://doi.org/10.1393/ncc/i2024-24378-2>.
9. McDonald, A.D.; Febbraro, M.; Asaadi, J.; Havener, C.C. Development of a pulsed vacuum ultraviolet light source with adjustable intensity. *Rev. Sci. Instrum.* **2022**, *93*, 053103, [arXiv:physics.ins-det/2111.06448]. <https://doi.org/10.1063/5.0081175>.
10. eSource Optics. 25125FNB (VUV Optical Bandpass Filter). last access: 04.07.2025.
11. Matsusada. INPUT/OUTPUT PROPORTIONAL HIGH VOLTAGE POWER SUPPLY. last access: 04.07.2025.
12. Kramida, A., Ralchenko, Yu., Reader, J. and NIST ASD Team (2024). NIST Atomic Spectra Database (version 5.12). *National Institute of Standards and Technology, Gaithersburg, MD*. **2025**. <https://doi.org/10.18434/T4W30F>.

**Disclaimer/Publisher's Note:** The statements, opinions and data contained in all publications are solely those of the individual author(s) and contributor(s) and not of MDPI and/or the editor(s). MDPI and/or the editor(s) disclaim responsibility for any injury to people or property resulting from any ideas, methods, instructions or products referred to in the content.